# Transition of Linear Polymer Dimension from Θ to Collapsed Regime. 2. Polystyrene/Methyl Acetate System

**Benjamin Chu,* I. H. Park, Q.-W. Wang,† and C. Wu**

*Department of Chemistry, State University of New York at Stony Brook, Long Island, New York 11794-3400.* *Received March 27, 1987*

ABSTRACT: We investigated the coil-to-globule transition of several narrow molecular weight distribution polystyrene samples with $M_w$ ranging from $2.0 \times 10^6$ to $8.6 \times 10^6$ g/mol in methyl acetate (solvent) both below the upper Θ temperature ($\Theta_U$ = 43 °C) and above the lower Θ temperature ($\Theta_L$ = 114 °C) using laser light scattering. The collapsed states based upon the static size (i.e., the radius of gyration $R_g$) were observed for the first time above the $\Theta_L$ temperature as well as below the $\Theta_U$ temperature. As the hydrodynamic size (i.e., the effective hydrodynamic radius, $R_h$) approaches the collapsed regime more slowly with temperature changes than the static size, the collapsed states based on hydrodynamic size could not be achieved in the polystyrene/methyl acetate (PS/MA) system by using the available instrumentation. We compared master curves obtained above the $\Theta_L$ temperature in the PS/MA system with 1 wt % antioxidant (2,6-di-*tert*-butyl-4-methylphenol) and below the $\Theta_U$ temperature in the PS/MA system with/without 1 wt % antioxidant in plots of $\alpha_s|\tau|M_w^{1/2}$ versus $|\tau|M_w^{1/2}$, where $\alpha_s[\equiv R_g(t)/R_g(\Theta)]$ is the expansion factor and $\tau$ [$\equiv T - \Theta/\Theta$] is the reduced temperature. We tried to interpret the difference in the asymptotic height for the collapsed regime of each system in terms of ($A^*N_1$), where $A^*$ is a proportional constant between number of monomers in one temperature blob ($N_c$) and the inverse square of reduced temperature ($\tau$) with $N_c = A^*\tau^{-2}$ and $N_1$ is the number of monomers in a statistical segment. Our experimental results showed that the $A^*$ parameter depends strongly upon the chemical nature of the solvent as well as the solvent quality (e.g., good or poor).

## I. Introduction

Theories[1-5] of polymer solution thermodynamics in which the free volume effects were taken into account could predict successfully the existence of both the upper critical solution temperature (UCST) and the lower critical solution temperature (LCST). Thus, in many polymer/solvent systems, phase separation occurs not only below UCST but also above LCST which often appears near the gas–liquid critical temperature of the solvent. The phase diagram of polymer solutions has been classified into two types of cloud-point curves. With increasing molecular weights, both the upper critical mixing point (UCP) and the lower critical mixing point (LCP) move toward lower concentrations. On the temperature axis, UCP moves up while LCP moves down with increasing molecular weights. Finally, UCP and LCP respectively coincide with the Flory $\Theta_U$ and $\Theta_L$ temperatures (simply denoted as $\Theta_U$ and $\Theta_L$) at infinite molecular weight and zero concentration. Until now, all existing coil-to-globule transition data[6-18] (including paper 1[19]) were obtained below the $\Theta_U$ temperature. However, there exists also another globular state which can be approached by increasing the temperature above the $\Theta_L$ temperature. It will be interesting to compare these two coil-to-globule transitions below the UCST and above the LCST in one system.

S. Saeki et al.[20] and K. Kubota et al.[21] reported that the polystyrene/methylacetate (PS/MA) system has two convenient Θ temperatures at 43 and 114 °C, which are accessible experimentally. Degradation of polymer chains can be reduced if not inhibited completely for time periods of ~12 h at 120 °C by adding ~1 wt % of an antioxidant. Therefore, the PS/MA system was chosen as the second model polymer solution not only to confirm the nature of the coil-to-globule transition of PS in cyclohexane but also to examine the contraction of polymer coils by enthalpy and entropy changes.[5]

## II. Theoretical Background

In paper 1,[19] we have expressed and discussed all of the equations used in this paper. The purpose of this section is to summarize the equations used to express polymer dimensions in the globule state, as well as relations between static and dynamic light scattering and the measured parameters needed in the discussion of our results.

**IIa. Polymer Dimensions in the Collapsed Regime.** In a polymer solution, when the temperature is decreased below $\Theta_U$ (or increased above $\Theta_L$), intramolecular interactions become more attractive and the polymer coil contracts. This contraction can be described by using the modified Flory equation[22,23] in terms of an expansion factor $\alpha$ [$\equiv(R(T)/R(\Theta)$]

$$\alpha^5 - \alpha^3 - \frac{w}{\alpha^3 a^6} = \frac{3}{2}\frac{vN^{1/2}}{a^3} \tag{1}$$

where $v$ and $w$ are respectively the binary and ternary cluster integral and $N$ is the number of monomer units, each of length $a$, in a polymer coil. Here, the excluded volume parameter $v$ is proportional to one monomer volume $a^3$ and is expressed[24] in terms of a reduced temperature $\tau$ ($\equiv T/\Theta - 1$). Near the Θ-temperature,

$$v \sim a^3\tau \tag{2}$$

In the temperature range $T < \Theta_U$ (or $T > \Theta_L$), where attractive interactions dominate, $\alpha$ becomes smaller than 1. From eq 1, $\alpha$ behaves like $(|\tau|N^{1/2})^{-1/3}$ when $\alpha \ll 1$, provided that $w$ remains constant over the temperature range of our investigation. It means that the chain is collapsed and its volume is proportional to $N$ (or the size $R \sim N^{1/3}$).

The crossover behavior between the Θ temperature and the collapsed regime may be predicted by replacing the exponent $\nu = {}^3/_5$ with $\nu = {}^1/_3$ in eq 3 and 4, which was used for describing the cross-over behavior from the Θ temperature to the good solvent limit. Here eq 3 and 4[24,25]

$$\alpha_s^2(x) = x^2(3 - 2x) + 6x^{1-2\nu}\left[\frac{1 - x^{2\nu+1}}{2\nu + 1} - \frac{1 - x^{2(\nu+1)}}{2(\nu + 1)}\right] \tag{3}$$

$$\alpha_h(x) = \frac{4}{x^{1/2}}\left[2(3 - x) + 3\left(\frac{x^{\nu-1} - 1}{1 - \nu} - \frac{x^{\nu-1} - x}{2 - \nu}\right)\right]^{-1} \tag{4}$$

express the expansion factors $\alpha_s$ of the radius of gyration ($R_g$) and $\alpha_h$ of the hydrodynamic radius ($R_h$) in terms of $x$ ($=N_c/N$) where $N_c$ is the number of monomers in one

† Present address: Department of Chemistry, Peking University, Beijing, People's Republic of China.

0024-9297/87/2220-2833$01.50/0 

temperature blob. The relation between the theoretical blob parameter ($N/N_c$) and the experimentally measurable quantity $|\tau|M_w^{1/2}$ can be written[24] as

$$N/N_c = \frac{\tau^2 M}{M_0(A^*N_1)} \quad (5)$$

where $M_0$ is the molecular weight of one monomer segment and $N_1$ is the number of monomer in a statistical segment. The prefactor ($A^*N_1$) can be determined from a comparison of theory and experiment. In the asymptotic limit ($x \ll 1$) and with $\nu = {}^1/_3$, one has

$$\alpha_s = 1.161(N/N_c)^{1/6} \quad \text{(poor solvent)} \quad (6)$$

$$\alpha_h = 1.481(N/N_c)^{1/6} \quad \text{(poor solvent)} \quad (7)$$

When we reach the collapsed regime, we can set the plateau height to be $h$ in a plot of $\alpha^3|\tau|M_w^{1/2}$ versus $|\tau|M_w^{1/2}$. Then, for the static case, by combining eq 5 and 6, we get

$$(A^*N_1) = h^2/(2.45M_0) \quad (8)$$

Equation 8 is independent of molecular weight, but may depend on polymer flexibility and nature of the solvent.

**IIb. Intensity of Scattered Light.**[26] The excess Rayleigh ratio, $R_{vv}$ ($cm^{-1}$), at a finite scattering angle $\theta$ in a dilute solution of concentration $C$ ($g/cm^3$) has the approximate form

$$\frac{HC}{R_{vv}} \simeq \frac{1}{M_w P(K)} + 2A_2C \quad (9)$$

where $H$ (mol $cm^2/g^2$) is equal to $4\pi^2n^2(dn/dC)^2/(N_A\lambda_0^4)$ with $n$, $N_A$, $\lambda_0$, and $dn/dC$ being respectively the refractive index, Avogadro's number, the wavelength of incident light in vacuo, and the refractive index increment. Subscripts vv indicate that both the incident and the scattered light are polarized vertically. $A_2$ (mol $cm^3/g^{-2}$) is the second virial coefficient and K [$=(4\pi n/\lambda_0)\sin(\theta/2)$] is the magnitude of the momentum transfer vector. $P(K)$ is a form factor which is related to the interference effect in a single polymer chain and can be expressed as

$$P^{-1}(K) = [1 + (KR_g)^2/3] \quad \text{(Zimm plot)} \quad (10a)$$

$$P^{-1}(K) = [1 + (KR_g)^2/6]^2 \quad \text{(Berry plot)} \quad (10b)$$

**IIc. Characteristic Line Width of Scattered Light.**[27,28] The intensity–intensity time correlation function $G^{(2)}(t)$ [$=\langle I(0)I(t)\rangle$] has the form:

$$G^{(2)}(t) = A(1 + b|g^{(1)}(t)|^2) \quad (11)$$

where $A$ and $b$ are respectively the base line and the coherence factor and $g^{(1)}(t)$ is the normalized correlation function of scattered electric field.

For a system with multiple characteristic line widths, $|g_1(t)|$ becomes

$$|g^{(1)}(t)| = \int_0^\infty G(\Gamma)\exp(-\Gamma t)\,d\Gamma \quad (12)$$

where $G(\Gamma)$ is the normalized characteristic line width distribution. At finite $K$ and finite $C$, the average characteristic line width $\bar{\Gamma}$ ($=\int_0^\infty G(\Gamma)\Gamma\,d\Gamma$) can be expressed[29] as

$$\bar{\Gamma}/K^2 \simeq \bar{D}_0(1 + f(KR_g)^2)(1 + k_dC) \quad (13)$$

where $k_d$ and $f$ are, respectively, the second virial coefficient for diffusion and a dimensionless constant that depends upon chain structure, polydispersity, and solvent quality. The $z$-average translational diffusion coefficient at infinite dilution ($\bar{D}_0$) can be converted to the hydrodynamic radius ($R_h$) by using the Stokes–Einstein equation

$$R_h = k_BT/(6\pi\eta\bar{D}_0) \quad (14)$$

**Table I**
**Comparison of the Effect of Antioxidant 2,6-Di-*tert*-butyl-4-methylphenol at High Temperature ($T$ = 120 °C) in the PS ($M_w = 17.5 \times 10^6$ g/mol)/MA System**

| amt added, wt % | $M_w(12)/M_w(0)$[a] | $R_g(12)/R_g(0)$[b] |
|---|---|---|
| 0.005 | 0.77 | 0.94 |
| 0.05 | 0.79 | 0.91 |
| 0.5 | 0.95 | 1.05 |

[a] Ratio of the molecular weight after 12 h to that at time $t$ = 0. [b] Ratio of the radius of gyration after 12 h to that at time $t$ = 0.

## III. Experimental Methods

Three narrow molecular weight distribution (MWD) polystyrene samples were used. Their molecular weights and indices of polydispersity were $M_w = 2.0 \times 10^6$ g/mol and $M_w/M_n = 1.1$ for sample code 2N, $M_w = 4.6 \times 10^6$ g/mol and $M_w/M_n = 1.14$ for sample code 4N, and $M_w = 8.6 \times 10^6$ g/mol and $M_w/M_n = 1.26$ for sample code 8N. Sample 2N was purchased from Waters, while samples 4N and 8N were purchased from Toyo Soda. Methyl acetate solvent was purified by drying overnight in anhydrous $MgSO_4$ and subsequent distillation under $P_2O_5$ before use. A mother solution with a concentration of $\sim 5 \times 10^{-4}$ g/g was prepared and was diluted to the order of $CM_w \sim 10$ $g^2$ $cm^{-3}$ $mol^{-1}$ for light scattering experiments. In this concentration range, the correction due to finite concentration in the determination of $R_g$ and $R_h$ was always negligible.[19] In order to prevent the degradation of polymer at high temperatures, we added an antioxidant (2,6-di-*tert*-butyl-4-methylphenol) to all our light scattering samples for high-temperature measurements. For comparison of effect of antioxidant, we also performed the following preliminary experiment. Three PS ($M_w = 17.5 \times 10^6$ g/mol, $C = 8 \times 10^{-6}$ g/g)/MA solutions with 0.005, 0.05, and 0.5 wt % of antioxidant, respectively, were kept at 120 °C for 12 h. Molecular weights and sizes of the three solutions were compared with the same system before prolonged heating at the same temperature. The light scattering results are listed in Table I. The solution with 0.5 wt % antioxidant showed no deterioration. Thus, all solutions for experiments above the $\Theta_L$ temperature were prepared by adding up to 1 wt % antioxidant. The $\Theta_U$ and $\Theta_L$ temperatures of PS/MA with 1 wt % antioxidant (simply denoted as PS/MA(1 wt %)) were measured experimentally. Figure 1 shows plots of the second virial coefficient $A_2$ versus temperature. In these plots, the temperature at which $A_2 = 0$ was defined as our $\Theta$ temperature. The $\Theta_U$ and $\Theta_L$ temperatures of the PS/MA(1 wt %) were 43 and 114 °C, respectively. The new $\Theta$ temperatures for the PS/MA(1 wt %) system were essentially the same as those of the original PS/MA system within experimental error limits (±0.5 °C).

The refractive index increment $(dn/dC)_T$ for the PS/MA system was measured with a Brice Phoenix differential refractometer at two different temperatures. The values were respectively 0.243 and 0.236 $cm^3/g$ at $\lambda_0$ = 436 and 546 nm and 25 °C and 0.247 and 0.240 $cm^3/g$ at the corresponding wavelengths and 43 °C. The refractive index of methyl acetate at 25 °C was 1.3671 and 1.3622 at $\lambda_0$ = 436 and 546 nm, respectively. The refractive index of methyl acetate at high temperatures was calculated by using the temperature coefficient of refractive index of MA to be $-5.0 \times 10^{-4}$/deg. The variation of refractive index for a temperature change of 80 °C was only less than 3%. Also, the refractive index of methyl acetate with 1 wt % antioxidant was used without further correction in comparison with that of the pure solvent, since the refractive index correction due to the antioxidant is of the order of 0.1%. The viscosity of methyl acetate solvent was calculated by using eq 15,[31] where $\eta$ (centipoise) is

$$\eta = (57.4)/(154.5 + T)^{1.864} \quad \text{(for MA)} \quad (15)$$

the solvent viscosity at temperature $T$ expressed in degrees Celsius. Methods of data analysis have been reported in detail in paper 1.[19]

**Table II**
**$R_g$ and $R_h$ in the PS/MA System with/without 1 wt % Antioxidant at $\Theta_U$ and $\Theta_L$ Temperatures**

| system | sample | $M_w \times 10^{-6}$, g/mol | $R_g$, nm[a] | $R_h$, nm[b] | $R_g^2/M_w$[c] | $R_h^2/M_w$,[c] | $R_h/R_g$ |
|---|---|---|---|---|---|---|---|
| PS/MA | 2N | 2.0 | 41.8 | 29.7 | 8.74 | 4.41 | 0.71 |
| $\Theta_U$ = 43 °C | 4N | 4.6 | 64.7 | 45.5 | 9.10 | 4.50 | 0.70 |
| PS/MA(1 wt %) | 4N | 4.6 | 65.1 | 48.3 | 9.21 | 5.07 | 0.74 |
| $\Theta_U$ = 43 °C | 8N | 8.6 | 92.8 | 66.2 | 10.0 | 5.10 | 0.71 |
| PS/MA(1 wt %) | 4N | 4.6 | 59.9 | | 7.80 | | |
| $\Theta_L$ = 114 °C | 8N | 8.6 | 86.7 | | 8.74 | | |

[a] $R_g$ could be determined to about ±3%. [b] $R_h$ could be determined to about ±2%. [c] Unit = $10^{-8}$ cm² mol/g.

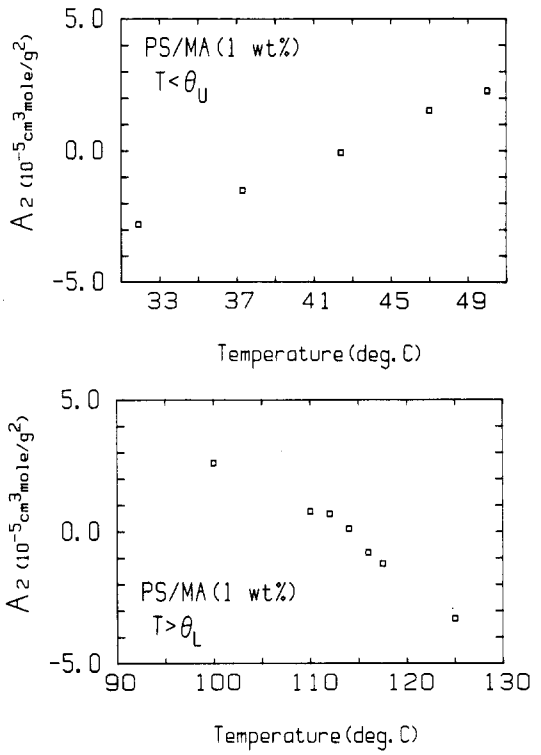


**Figure 1.** Variation of second virial coefficient $A_2$ as a function of temperature (°C) in the polystyrene ($M_w$ = 2.33 × $10^5$ g/mol)/methyl acetate system with 1 wt % antioxidant (2,6-di-*tert*-butyl-4-methylphenol). (Top) The $\Theta_U$ temperature of the PS/MA(1 wt %) system could be estimated to be 43 °C. (Bottom) The $\Theta_L$ temperature of PS/MA(1 wt %) could be estimated to be 114 °C.

## IV. Results and Discussion

**IVa. PS/MA below the $\Theta_U$ Temperature.** The measured values of $R_g$ and $R_h$ of several polystyrene samples in MA with/without 1 wt % antioxidant at $\Theta_U$ and $\Theta_L$ temperatures are listed in Table II. By comparing sizes of the polymer chain at the Θ temperature (referred to as the Θ size) of several different systems, we made the following observations: (1) The 1 wt % antioxidant does not affect the Θ sizes or the Θ temperature in the PS/MA system. (2) The Θ sizes in the PS/MA system appear to be comparable to those reported in the literature.[17,30] (3) In the PS/MA system with 1 wt % antioxidant the Θ size at $\Theta_L$ temperature (114 °C) is smaller by ~8% than that at $\Theta_U$ temperature (43 °C). Since the monomer bonds can rotate more freely on the joint points at the high Θ temperature ($\Theta_L$) than at the low Θ temperature ($\Theta_U$), the $R_g(\Theta_L)$ is smaller than $R_g(\Theta_U)$.

The radii of gyration and hydrodynamic radii of PS/MA with/without 1 wt % antioxidant below the $\Theta_U$ temperature are listed, respectively, in Tables III, IV, V, and VI. Figure 2 shows the variation of $\alpha_s^3|\tau|M_w^{1/2}$ of the static sizes with respect to the scaled reduced temperature $|\tau|M_w^{1/2}$. Data for the PS/CY system were also plotted in the same figure for comparison. The collapsed state based on the static size was achieved in both PS/MA and PS/MA(1 wt %) systems. However, the asymptotic height at the plateau region depends upon the chemical nature of each system as illustrated in Figure 2. The PS/MA(1 wt %)

**Table III**
**Radii of Gyration of Polystyrene in Methyl Acetate below the $\Theta_U$ Temperature**

| $10^{-6}M_w$, g/mol | $10^6C$, g/g | temp, °C | $R_g$, nm | $\alpha_s$ | $\lvert\tau\rvert M_w^{1/2}$[a] | $\alpha_s^3\lvert\tau\rvert M_w^{1/2}$[a] |
|---|---|---|---|---|---|---|
| 2.0 | 5.8 | 43.0 | 41.8 | 1.00 | 0 | 0 |
| (2N) | | 40.0 | 41.6 | 0.995 | 13.4 | 13.2 |
| | | 37.0 | 40.9 | 0.978 | 26.9 | 25.2 |
| | | 35.0 | 39.5 | 0.945 | 35.8 | 30.2 |
| | | 32.0 | 37.8 | 0.904 | 49.3 | 36.4 |
| | | 29.0 | 36.8 | 0.880 | 62.7 | 42.7 |
| | | 27.0 | 36.6 | 0.876 | 71.7 | 48.2 |
| | | 25.0 | 35.4 | 0.847 | 80.6 | 49.0 |
| 4.6 | 3.2 | 43.0 | 65.8 | 1.00 | 0 | 0 |
| (4N) | | 38.5 | 62.1 | 0.944 | 20.3 | 17.1 |
| | | 36.5 | 60.6 | 0.921 | 44.1 | 34.5 |
| | | 33.5 | 58.4 | 0.888 | 64.5 | 45.2 |
| | | 32.0 | 57.3 | 0.871 | 74.7 | 49.4 |
| | | 31.0 | 56.4 | 0.857 | 81.5 | 51.3 |
| | | 30.0 | 54.0 | 0.821 | 88.3 | 48.9 |
| 4.6 | 2.4 | 43.0 | 63.6 | 1.00 | 0 | 0 |
| (4N) | | 37.0 | 58.2 | 0.916 | 40.7 | 31.3 |
| | | 35.5 | 56.9 | 0.894 | 50.9 | 36.4 |
| | | 34.0 | 56.4 | 0.888 | 61.1 | 42.8 |
| | | 32.5 | 56.0 | 0.881 | 71.3 | 48.8 |
| | | 31.0 | 54.5 | 0.858 | 81.5 | 51.5 |
| | | 29.5 | 53.2 | 0.837 | 91.7 | 53.7 |
| | | 28.0 | 50.5 | 0.799 | 102 | 52.0 |

[a] $M_w$ in units of g mol$^{-1}$.

**Table IV**
**Hydrodynamic Radii of Polystyrene in Methyl Acetate below the $\Theta_U$ Temperature**

| $10^{-6}M_w$, g/mol | $10^6C$, g/g | temp, °C | $R_g$, nm | $\alpha_h$ | $\lvert\tau\rvert M_w^{1/2}$[a] | $\alpha_h^3\lvert\tau\rvert M_w^{1/2}$[a] |
|---|---|---|---|---|---|---|
| 2.6 | 3.0 | 43.0 | 29.2 | 1.00 | 0 | 0 |
| (2N) | | 40.0 | 29.3 | 1.00 | 13.4 | 13.4 |
| | | 37.0 | 28.9 | 0.990 | 26.9 | 26.1 |
| | | 32.0 | 27.8 | 0.952 | 40.3 | 34.8 |
| | | 27.0 | 26.9 | 0.921 | 71.6 | 55.9 |
| | | 24.0 | 26.8 | 0.917 | 85.0 | 65.5 |
| | | 22.0 | 26.2 | 0.897 | 94.0 | 67.8 |
| 4.6 | 2.0 | 43.0 | 45.5 | 1.00 | 0 | 0 |
| (4N) | | 42.0 | 45.1 | 0.991 | 6.80 | 6.62 |
| | | 41.0 | 45.7 | 1.00 | 13.6 | 13.8 |
| | | 40.0 | 45.7 | 1.00 | 20.4 | 20.6 |
| | | 38.0 | 45.3 | 0.996 | 33.9 | 33.5 |
| | | 37.0 | 44.4 | 0.976 | 40.7 | 37.8 |
| | | 36.0 | 43.8 | 0.963 | 47.5 | 42.4 |
| | | 35.0 | 43.2 | 0.949 | 54.3 | 46.4 |
| | | 34.0 | 43.2 | 0.949 | 61.1 | 52.2 |
| | | 33.0 | 41.9 | 0.921 | 67.9 | 53.0 |
| | | 32.0 | 41.8 | 0.919 | 74.7 | 58.0 |
| | | 31.0 | 41.3 | 0.908 | 81.4 | 60.9 |
| | | 30.0 | 41.0 | 0.901 | 88.2 | 64.5 |
| | | 29.0 | 40.1 | 0.881 | 95.0 | 65.0 |
| | | 28.0 | 39.7 | 0.872 | 102 | 67.5 |

[a] $M_w$ in units of g mol$^{-1}$.

**Table V**
**Radii of Gyration of Polystyrene in Methyl Acetate with 1 wt % Antioxidant below the $\Theta_U$ Temperature**

| $10^{-6}M_w$, g/mol | $10^6C$, g/g | temp, °C | $R_g$, nm | $\alpha_s$ | $\lvert\tau\rvert M_w^{1/2a}$ | $\alpha_s^3\lvert\tau\rvert M_w^{1/2a}$ |
|---|---|---|---|---|---|---|
| 4.6 | 36.0 | 43.0 | 65.6 | 1.00 | 0 | 0 |
| (4N) | | 41.5 | 63.8 | 0.973 | 10.2 | 9.40 |
| | | 38.0 | 62.1 | 0.947 | 33.9 | 28.0 |
| | | 34.5 | 61.1 | 0.931 | 57.7 | 46.6 |
| | | 31.5 | 59.4 | 0.905 | 78.1 | 57.9 |
| | | 30.0 | 57.1 | 0.870 | 88.2 | 58.1 |
| | | 28.5 | 56.9 | 0.867 | 98.5 | 64.2 |
| | | 26.9 | 55.9 | 0.852 | 109 | 67.6 |
| | | 25.5 | 54.7 | 0.834 | 119 | 68.9 |
| 4.6 | 9.6 | 43.0 | 63.8 | 1.00 | 0 | 0 |
| (4N) | | 30.0 | 56.6 | 0.887 | 88.2 | 61.5 |
| | | 28.0 | 55.4 | 0.868 | 102 | 66.6 |
| | | 26.0 | 53.6 | 0.840 | 115 | 68.4 |
| | | 24.0 | 52.3 | 0.820 | 129 | 71.1 |
| 4.6 | 4.0 | 43.0 | 64.6 | 1.00 | 0 | 0 |
| (4N) | | 29.0 | 57.4 | 0.889 | 95.1 | 66.8 |
| | | 27.0 | 54.5 | 0.843 | 109 | 65.2 |
| | | 25.0 | 53.5 | 0.828 | 122 | 69.4 |
| | | 23.0 | 51.7 | 0.800 | 136 | 69.6 |
| 8.6 | 21.2 | 43.0 | 92.4 | 1.00 | 0 | 0 |
| (8N) | | 41.5 | 89.7 | 0.971 | 13.9 | 12.7 |
| | | 39.6 | 88.7 | 0.960 | 31.6 | 28.0 |
| | | 37.6 | 85.7 | 0.927 | 50.1 | 39.9 |
| | | 35.7 | 84.8 | 0.918 | 67.7 | 52.3 |
| | | 33.7 | 82.6 | 0.894 | 86.3 | 61.7 |
| | | 32.8 | 82.0 | 0.887 | 94.7 | 66.1 |
| | | 31.8 | 80.0 | 0.866 | 104 | 67.5 |
| | | 30.8 | 79.0 | 0.855 | 113 | 70.8 |
| | | 29.8 | 77.7 | 0.841 | 123 | 72.8 |
| | | 28.9 | 74.9 | 0.811 | 131 | 69.7 |
| | | 27.9 | 73.4 | 0.794 | 140 | 70.2 |
| 8.6 | 6.4 | 43.0 | 94.1 | 1.00 | 0 | 0 |
| (8N) | | 32.8 | 83.8 | 0.891 | 94.7 | 67.0 |
| | | 30.8 | 81.4 | 0.865 | 113 | 73.3 |
| | | 28.9 | 77.5 | 0.823 | 131 | 72.9 |
| | | 26.9 | 73.6 | 0.782 | 149 | 71.4 |
| | | 25.0 | 71.2 | 0.757 | 167 | 72.4 |

[a] $M_w$ in units of g mol$^{-1}$.

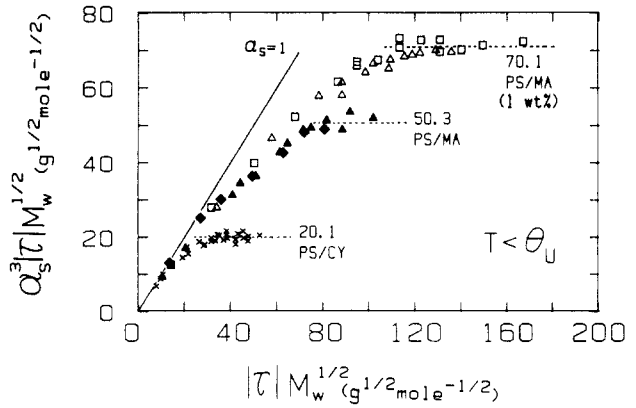


**Figure 2.** Variation of scaled expansion factor $\alpha_s^3|\tau|M_w^{1/2}$ of static size as a function of scaled reduced temperature $|\tau|M_w^{1/2}$ at $T < \Theta_U$. Open and filled symbols indicate PS/MA(1 wt %) with data listed in Table V and PS/MA with data listed in Table III, respectively. (Diamonds) sample $2N$ ($M_w = 2.0 \times 10^6$ g/mol); (triangles) sample $4N$ ($M_w = 4.6 \times 10^6$ g/mol); (squares) sample $8N$ ($M_w = 8.6 \times 10^6$ g/mol). The static size data of polystyrene/cyclohexane (PS/CY) system (×) were also presented for comparison.[19] The dashed lines denote the asymptotic collapsed regimes and the numbers are the asymptotic heights in the collapsed regime in units of g$^{1/2}$ mol$^{-1/2}$. It should be noted that the scaled curves were obtained by using PS with different molecular weights and at different concentrations.

system has the largest value and the order is as follows: system (asymptotic height) PS/CY (20.1) < PS/MA (50.3) < PS/MA(1 wt %) (70.1).

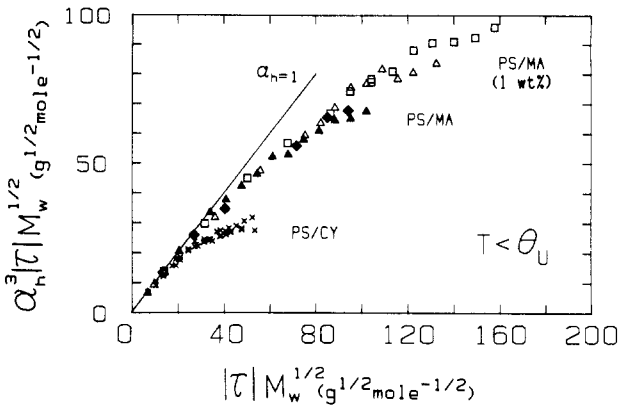


**Figure 3.** Variation of scaled expansion factor $\alpha_h^3|\tau|M_w^{1/2}$ of hydrodynamic size as a function of scaled reduced temperature $|\tau|M_w^{1/2}$ at $T < \Theta_U$. Open and filled symbols indicate PS/MA(1 wt %) with data listed in Table VI and PS/MA with data listed in Table IV. (Diamonds) sample $2N$ ($M_w = 2.0 \times 10^6$ g/mol); (triangles) sample $4N$ ($M_w = 4.6 \times 10^6$ g/mol); (squares) sample $8N$ ($M_w = 8.6 \times 10^6$ g/mol). The hydrodynamic size data of the PS/CY system (×) were also presented for comparison.[19] The collapsed regime based upon hydrodynamic size has not yet been reached in this experiment. It should be noted that the scaled curves were obtained by using PS with different molecular weights and at different concentrations. With imagination, one may see a possible leveling in the scaled curves suggesting that we have almost reached the collapsed regime based upon the hydrodynamic size.

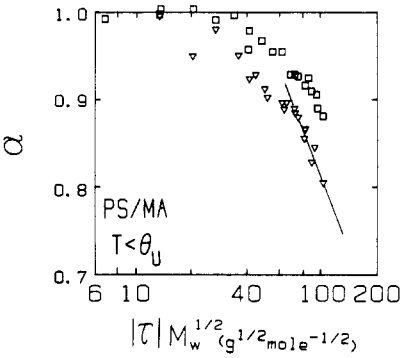


**Figure 4.** log–log plots of expansion factor $\alpha$ versus scaled reduced temperature $|\tau|M_w^{1/2}$ in PS/MA at $T < \Theta_U$. (▽) Expansion factor of static size (e.g., $R_g$ from Table V), $\alpha = \alpha_s$; (□) expansion factor of hydrodynamic size (e.g., $R_h$ from Table IV), $\alpha = \alpha_h$. Solid line denotes an asymptotic slope of 0.29 ± 0.06 in the collapsed regime based upon the static $R_g$ values. $\Theta_U$ = 43 °C. Note the rate of change of $\alpha_h$ suggesting that we have almost reached the collapsed regime based on hydrodynamic size.

The PS/MA system has a much wider Θ regime than the PS/CY system. This trend was already observed by Kubota et al.[21] in the PS ($M_w = 1.79 \times 10^5$ g/mol)/MA system, where the two Θ regimes ($\Theta_U$ and $\Theta_L$) virtually overlapped.

Measurements could be performed without any aggregation at a lower temperature (by ~5 °C in sample 4N) in PS/MA(1 wt %). This behavior suggests that the $\Theta_U$ coexistence curve seems to have a steeper slope in the low polymer concentration side of the cloud-point curve by adding the 1 wt % antioxidant.

In Figure 3, $\alpha_h^3|\tau|M_w^{1/2}$ increased continuously with increasing scaled reduced temperature ($|\tau|M_w^{1/2}$), never reaching a plateau. The maximum values obtained in PS/MA and PS/MA(1 wt %) systems were respectively ~72 and ~96 g$^{1/2}$ mol$^{-1/2}$, corresponding to ~68% of the theoretical asymptotic heights (PS/MA, 2.08 × 50.3 ~ 105; PS/MA(1 wt %), 2.08 × 70.1 ~ 146) based on hydrodynamic size. These theoretical values were estimated from the asymptotic heights based on the static size (see Figure

**Table VI**
**Hydrodynamic Radii of Polystyrene in Methyl Acetate with 1 wt % Antioxidant below the $\Theta_U$ Temperature**

| $10^{-6}M_w$, g/mol | $10^6C$, g/g | temp, °C | $R_h$, nm | $\alpha_h$ | $\lvert\tau\rvert M_w^{1/2}$ [a] | $\alpha_h^3\lvert\tau\rvert M_w^{1/2}$ [a] |
|---|---|---|---|---|---|---|
| 4.6 | 9.6 | 43.0 | 48.2 | 1.00 | 0 | 0 |
| (4N) | | 40.9 | 47.1 | 0.978 | 14.3 | 13.4 |
| | | 37.7 | 46.3 | 0.960 | 36.0 | 31.9 |
| | | 34.8 | 45.7 | 0.948 | 55.7 | 47.5 |
| | | 31.9 | 44.5 | 0.924 | 75.3 | 59.4 |
| | | 30.0 | 44.3 | 0.920 | 88.2 | 68.7 |
| | | 28.0 | 43.9 | 0.910 | 102 | 76.7 |
| | | 26.0 | 42.4 | 0.879 | 115 | 78.4 |
| 4.6 | 4.0 | 43.0 | 48.5 | 1.00 | 0 | 0 |
| (4N) | | 41.6 | 48.2 | 0.994 | 9.5 | 9.3 |
| | | 30.9 | 44.5 | 0.918 | 82.1 | 63.5 |
| | | 29.0 | 44.9 | 0.926 | 95.0 | 75.4 |
| | | 27.0 | 44.1 | 0.909 | 109 | 81.6 |
| | | 25.0 | 42.2 | 0.870 | 122 | 80.5 |
| | | 23.5 | 41.6 | 0.858 | 132 | 83.6 |
| 8.6 | 21.2 | 43.0 | 65.1 | 1.00 | 0 | 0 |
| (8N) | | 41.5 | 65.1 | 1.00 | 13.9 | 13.9 |
| | | 39.6 | 63.9 | 0.981 | 31.6 | 29.8 |
| | | 37.6 | 62.8 | 0.965 | 50.1 | 45.0 |
| | | 35.7 | 61.4 | 0.943 | 67.7 | 56.8 |
| | | 33.7 | 59.8 | 0.918 | 86.3 | 66.8 |
| | | 31.8 | 59.0 | 0.906 | 104 | 77.3 |
| | | 29.8 | 58.3 | 0.896 | 123 | 88.1 |
| | | 27.9 | 56.4 | 0.866 | 140 | 91.0 |
| 8.6 | 6.4 | 43.0 | 66.6 | 1.00 | 0 | 0 |
| (8N) | | 32.8 | 61.5 | 0.922 | 94.7 | 74.2 |
| | | 30.8 | 59.6 | 0.894 | 113 | 80.9 |
| | | 28.9 | 59.0 | 0.885 | 131 | 90.6 |
| | | 26.9 | 56.8 | 0.852 | 149 | 92.4 |
| | | 26.0 | 56.4 | 0.847 | 158 | 95.9 |

[a] $M_w$ in units of g mol$^{-1}$.

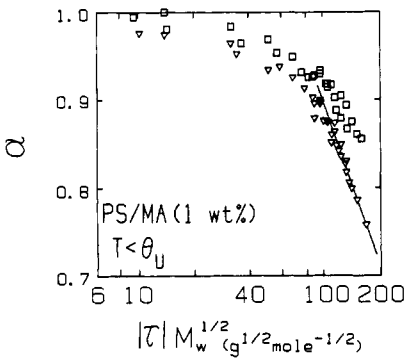


**Figure 5.** log–log plots of expansion factor $\alpha$ versus scaled reduced temperature $|\tau|M_w^{1/2}$ in PS/MA with 1 wt % antioxidant at $T < \Theta_U$. Symbols are the same in Figure 4. Data for $R_g$ are from Table V, and for $R_h$, Table VI. Solid line denotes an asymptotic slope of $-0.31 \pm 0.03$ in the collapsed regime based upon the static $R_g$ values. $\Theta_U$ = 43 °C. Note the rate of change of $\alpha_h$ suggesting that we have almost reached the collapsed regime based on hydrodynamic size.

2) by using eq 6 and 7 of the blob theory.

Figures 4 and 5 show log–log plots of expansion factors of both static and hydrodynamic sizes in PS/MA and PS/MA(1 wt %) as a function of the scaled reduced temperature $|\tau|M_w^{1/2}$. The static size has slopes of $-0.29 \pm 0.06$ and of $-0.31 \pm 0.03$, respectively, for PS/MA and PS/MA(1 wt %). However, the slope related to the hydrodynamic size did not reach the collapsed exponent of $-1/3$.

In Figure 6, the normalized ratio of $R_h/R_g$, which is related to the solvent permeability, increased very slowly with decreasing temperature. The limiting value (1.27) based on the blob theory could not yet be achieved. The low experimental value (1.19) implies that solvent molecules still permeate inside the collapsed coil (based on static size measurements) in the PS/MA system, similar

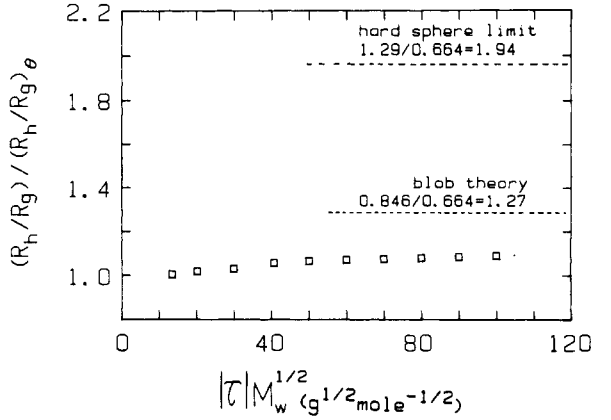


**Figure 6.** Variation of normalized $R_h/R_g$ ratio as a function of scaled reduced temperature ($|\tau|M_w^{1/2}$) in PS/MA with 1 wt % antioxidant at $T < \Theta_U$. Normalized ratio has increased only ~10% even at the collapsed regime (based upon the static $R_g$ values) and is far away from the value predicted by eq 6 and 7 based on the blob theory. $\Theta_U$ = 43 °C.

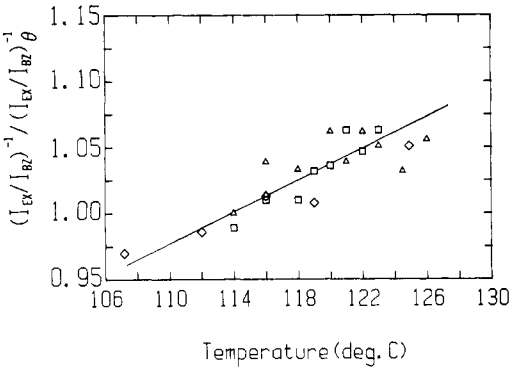


**Figure 7.** Normalized inverse scattered intensity versus temperature (°C) in PS/MA with 1 wt % antioxidant at $T > \Theta_L$. (Diamonds) Sample 2N ($M_w = 2.0 \times 10^6$ g/mol); (triangles) sample 4N ($M_w = 4.6 \times 10^6$ g/mol); (squares) sample 8N ($M_w = 8.6 \times 10^6$ g/mol). Data for samples 4N and 8N are listed in Table VII. Solid line denotes a temperature coefficient (~0.7%/°C) of normalized inverse scattered intensity based on a least-squares fitting of experimental data. $I_{EX}$ and $I_{BZ}$ are, respectively, the excess scattered intensity of polymer solution and the scattered intensity of benzene reference.

to the experimental behavior observed in the PS/CY system.[19]

**IVb. PS/MA above the $\Theta_L$ Temperature.** Although preliminary experiments already showed that the sample with 0.5 wt % antioxidant was not degraded for ~12 h at 120 °C, we reexamined whether or not the polymer chains became degraded during our experiments. As many physical constants for the polymer solution, such as the refractive index increment of PS/MA(1 wt %) near the $\Theta_L$ temperature, are not well-known at high temperatures, we monitored carefully the variation of the absolute scattered intensity with temperature. Figure 7 shows a plot of normalized inverse scattered intensities of several different molecular weight polystyrene samples with $M_w$ ranging from $2 \times 10^6$ to $8.6 \times 10^6$ g/mol as a function of temperature. By observing the reproducibility of the increasing rate of the inverse scattered intensity with respect to temperature (~0.7%/deg) for all polymer samples, we confirmed that our measurements with high molecular weight polystyrene samples did not show either degradation or aggregation during our experiments. The reason for this confirmation is as follows. Experiments have shown that low molecular weight PS samples (e.g., sample 2N) are not easily degradable. By using the low molecular weight PS as a base line with reproducible results of

**Table VII**
**Radii of Gyration of Polystyrene in Methyl Acetate with 1 wt % Antioxidant above the $\Theta_L$ Temperature**

| $10^{-6}M_w$, g/mol | $10^6C$, g/g | temp, °C | $R_g$, nm | $\alpha_s$ | $\lvert\tau\rvert M_w^{1/2}$ [a] | $\alpha_s^3\lvert\tau\rvert M_w^{1/2}$ [a] |
|---|---|---|---|---|---|---|
| 4.6 | 9.6 | 114.0 | 60.0 | 1.00 | 0 | 0 |
| (4N) | | 116.0 | 58.5 | 0.975 | 11.1 | 10.3 |
| | | 118.0 | 57.3 | 0.955 | 22.2 | 19.3 |
| | | 120.0 | 56.4 | 0.940 | 33.2 | 27.6 |
| | | 122.0 | 55.3 | 0.922 | 44.3 | 34.7 |
| | | 124.0 | 53.0 | 0.883 | 55.4 | 38.1 |
| 4.6 | 4.0 | 114.0 | 59.8 | 1.00 | 0 | 0 |
| (4N) | | 116.0 | 58.9 | 0.985 | 11.1 | 10.6 |
| | | 121.0 | 54.3 | 0.908 | 38.8 | 29.0 |
| | | 123.0 | 52.0 | 0.870 | 49.9 | 32.9 |
| | | 124.5 | 51.8 | 0.866 | 58.2 | 37.8 |
| | | 126.0 | 49.3 | 0.824 | 66.5 | 37.2 |
| 8.6 | 21.2 | 114.0 | 85.2 | 1.00 | 0 | 0 |
| (8N) | | 116.0 | 84.8 | 0.995 | 15.2 | 15.0 |
| | | 118.0 | 82.9 | 0.973 | 30.3 | 27.9 |
| | | 119.0 | 79.0 | 0.927 | 37.9 | 30.2 |
| | | 120.0 | 76.2 | 0.894 | 45.5 | 32.5 |
| | | 121.0 | 73.9 | 0.867 | 53.1 | 34.6 |
| | | 122.0 | 73.2 | 0.859 | 60.6 | 38.4 |
| | | 123.0 | 70.2 | 0.824 | 68.2 | 38.2 |
| 8.6 | 6.4 | 114.0 | 88.2 | 1.00 | 0 | 0 |
| (8N) | | 116.0 | 84.4 | 0.957 | 15.2 | 13.3 |
| | | 119.5 | 80.7 | 0.951 | 41.7 | 31.9 |
| | | 121.5 | 77.3 | 0.876 | 56.8 | 38.2 |
| | | 122.5 | 74.1 | 0.840 | 64.4 | 38.2 |
| | | 123.5 | 72.0 | 0.816 | 72.0 | 39.1 |
| | | 124.5 | 69.5 | 0.788 | 79.6 | 38.9 |
| | | 125.5 | 67.3 | 0.763 | 87.1 | 38.7 |

[a] $M_w$ in units of g mol$^{-1}$.

scattered intensity as a function of temperature from ~100 to 125 °C, we demonstrated that the high molecular weight PS samples (4N and 8N) showed similar trends. Higher molecular weight PS samples ($M_w \sim 2 \times 10^7$ g/mol) revealed changes and the results were discarded. Also, by reproducing the scattered intensity of our samples at the original starting temperature (usually 114 °C) after completion of all other measurements, we have proved that there was no degradation or phase separation during the course of our experiments. The high-temperature experiments were performed by using a laser power density of less than ~100 W/cm$^2$ in order to alleviate possible degradation due to high laser power density.[19] The measured $R_g$ and other values are listed in Table VII. Unfortunately, we did not have sufficient time to measure time correlation functions before sample deterioration at high temperatures because of the long accumulation time required.

We observed the collapsed regime of the static size above the $\Theta_L$ temperature as well as below the $\Theta_U$ temperature. The PS/MA(1 wt %) system above $\Theta_L$ had a smaller asymptotic height ($\alpha_s^3|\tau|M_w^{1/2} \sim 38.3$) when compared with those of the same system below $\Theta_U$ ($\alpha_s^3|\tau|M_w^{1/2} \sim 70.1$), as shown in Figure 8. Figure 9 shows a log–log plot of the expansion factor of the static size, $\alpha_s$, as a function of the scaled reduced temperature $|\tau|M_w^{1/2}$ at $T > \Theta_L$. The asymptotic slope (−0.32 ± 0.02, denoted by a solid line in Figure 9) of the static size agrees well with the theoretical exponent (−1/3) in the collapsed regime.

At $T < \Theta_U$ and $T > \Theta_L$, the measureable $\Delta T$ [$=|T - \Theta|$] range was smaller above $\Theta_L$ than below $\Theta_U$ using the same polymer solution concentration. For example, $\Delta T \sim 10$ °C for $T > \Theta_L$, but $\Delta T \sim 20$ °C for $T < \Theta_U$ for sample 4N at $C = 9.5 \times 10^{-6}$ g/g. This observation would imply that the two coexistence curves are not symmetrical with respect to the Θ-temperature axis.

We listed the values of the prefactor ($A^*N_1$) calculated from the measured asymptotic height of $\alpha_s^3|\tau|M_w^{1/2}$ in each

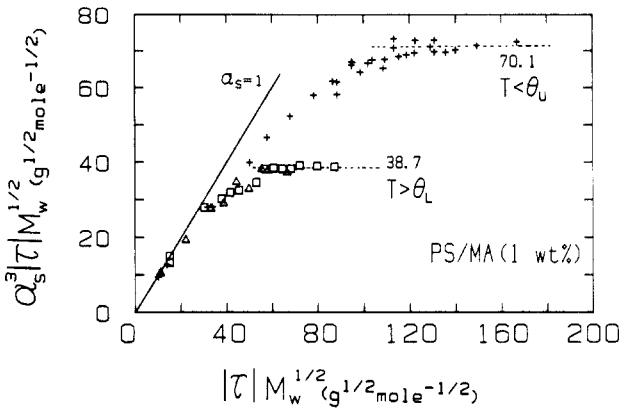


**Figure 8.** Variation of scaled expansion factor $\alpha_s^3|\tau|M_w^{1/2}$ of static size as a function of scaled reduced temperature $|\tau|M_w^{1/2}$ in PS/MA with 1 wt % antioxidant. (Triangles) Sample 4N ($M_w = 4.6 \times 10^6$ g/mol), (squares) sample 8N ($M_w = 8.6 \times 10^6$ g/mol). Data are listed in Table VII. The static size data obtained at $T < \Theta_U$ for the same system, as shown in Figure 2, are denoted by (+) in this figure for comparison purposes. The dashed lines denote the asymptotic collapsed regime and the numbers are the asymptotic heights in the collapsed regime in units of g$^{1/2}$ mol$^{-1/2}$.

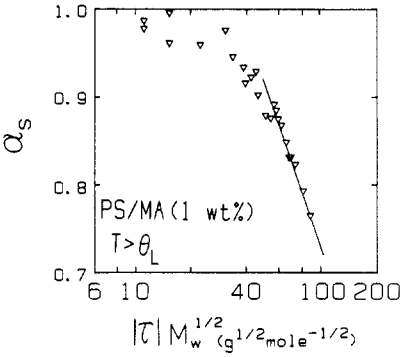


**Figure 9.** log–log plot of expansion factor $\alpha_s$ of static size versus scaled reduced temperature $|\tau|M_w^{1/2}$ in PS/MA with 1 wt % antioxidant at $T > \Theta_L$. Solid line denotes an asymptotic slope of −0.32 ± 0.02 in the collapsed regime based on the static $R_g$ values. $\Theta_L$ = 114 °C. Data are listed in Table VII.

system and the theoretical expectation $\alpha_s = 1.161(N/N_c)^{1/6}$ according to eq 8.

| system | $(A^*N_1)$ |
|---|---|
| PS/MA(1 wt %) for $T < \Theta_U$ (poor solvent) | 19 |
| PS/MA for $T < \Theta_U$ (poor solvent) | 9.9 |
| PS/MA(1 wt %) for $T > \Theta_L$ (poor solvent) | 5.8 |
| PS/CY for $T < \Theta_U$ (poor solvent) | 1.6 (ref 19) |
| PS/CY for $T > \Theta_U$ (good solvent) | ~4.0 (ref 24) |

Surprisingly, the value of the prefactor ($A^*N_1$) varied by a factor of more than ~10. The question is, why should there be such a big difference? First, let us assume that the number of monomers in one statistical length ($N_1$) remains insensitive to the solvent or the Θ temperature for a given polymer. As the parameter $N_1$ is related to the flexibility of the polymer backbone units, a decrease in Θ size indirectly implies a decrease in the magnitude of the $N_1$ parameter. For example, an extremely large value for the $N_1$ parameter corresponds to the polymer behaving more like a semiflexible chain. Based on the variation of ~10% in the Θ size for all the different systems, the assumption of a relatively constant value for the $N_1$ parameter, at least in the Θ region, is reasonable. Thus, the system dependence of the prefactor ($A^*N_1$) came mainly from the $A^*$ parameter rather than the $N_1$ parameter. The original blob theory predicted that $A^*$ ($=N_c\tau^2$) could be insensitive to the solvent nature and the structure of the

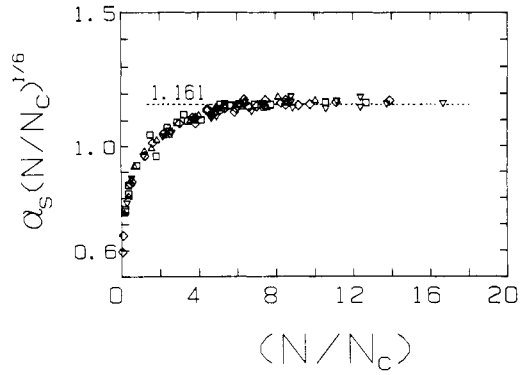


**Figure 10.** Universal plot of static size versus reduced blob parameter ($N/N_c$). All data obtained from different systems could be superposed on one curve. (Squares) PS/MA(1 wt %) at $T > \Theta_L$; (diamonds) PS/MA(1 wt %) at $T < \Theta_U$; (triangles) PS/MA at $T < \Theta_U$; (inverted triangles) PS/CY at $T < \Theta_U$. The static size data of PS/CY system were presented for comparison.[19] Data points reached the asymptotic collapsed value (1.161) predicted by eq 6 above $(N/N_c) > 5$. $(N/N_c)$ is the number of temperature blobs in a single polymer chain. It should be noted that we have used the $(A^*N_1)$ value for each system based on eq 8 and the experimental asymptotic height $h$.

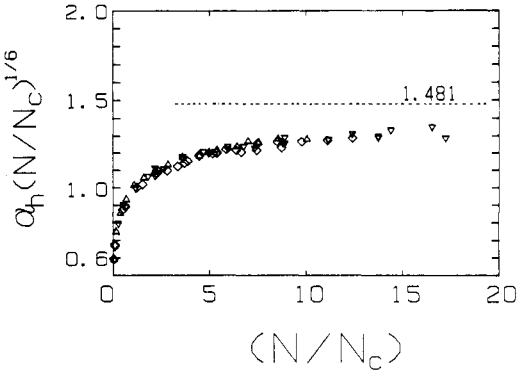


**Figure 11.** Universal plot of hydrodynamic size versus reduced blob parameter ($N/N_c$). Although all data obtained from different systems (including the use of the $(A^*N_1)$ value for each system as reported in Figure 10, based on static size) could be superposed on one curve, they did not reach the asymptotic collapsed value (1.481) predicted by eq 7. Symbols are the same in Figure 10. The hydrodynamic size data of the PS/CY system were presented for comparison.[19]

monomer units. Our experimental results showed that the $A^*$ parameter was very strongly dependent upon (i) the chemical nature of the system, e.g., in the PS/CY system, $A^*N_1 = 1.6$ for $T < \Theta_U$ and in the PS/MA system, $A^*N_1 = 9.9$ for $T < \Theta_U$, and/or (ii) the solvent quality, e.g., good or poor solvent for the PS/CY system where $A^*N_1 = 1.$ for $T < \Theta_U$ and $\sim 4$ for $T < \Theta_U$. Furthermore, it is surprising to find that for the PS/MA system at $T < \Theta_U$, $A^*N_1 = 9.9$ and 19 without and with 1 wt % antioxidant, even though $\Theta_U \sim 43$ °C and $R_g^2/M_w \sim 9 \times 10^{-18}$ cm$^2$ mol/g for the PS/MA system without and with 1 wt % antioxidant. Variations of $A^*N_1$ values with only a small change in solvent (i.e., addition of 1 wt % antioxidant) suggested that $A^*$ is very sensitive to the chemical nature of the solvent used. In this case, a slight change in the chemical nature of the solvent has changed the shape and the location of the coexistence curve and the ranges of $\Theta$ and globule regimes. Therefore, we suggest a reexamination of the $A^*$ parameter theoretically.

Figures 10 and 11 show plots of $\alpha(N/N_c)^{1/6}$ as a function of the reduced blob parameter $N/N_c$ for all known systems. In Figure 10, all data points are well superposed, not only in the collapsed regime ($N/N_c > 5$) but also in the crossover regime ($0 < N/N_c < 5$), indicating that a reduced blob parameter can be considered as a universal system-independent variable with regard to the contraction of polymer sizes even if it needs an empirically adjustable parameter ($A^*N_1$) between theory and experiments in the asymptotic collapsed regime.

## V. Conclusions

We observed the collapsed regimes based on the static size above the $\Theta_L$ temperature in the PS/MA (1 wt %) system as well as below the $\Theta_U$ temperature in PS/MA systems with and without addition of an antioxidant. The measurements represent the first experimental evidence for the existence of a collapsed regime above the $\Theta_L$ temperature.

The collapsed regimes based on the static size were observed in PS/CY and PS/MA systems but the collapsed regime based on the hydrodynamic size could not be reached in any system, partially due to the slower contraction of the hydrodynamic size over a broader temperature range, and partially due to our instrumental limitations requiring a finite polymer concentration not sufficiently dilute in order to avoid phase separation. More experiments with a very narrow MWD and high molecular weight polystyrene should permit us to observe the entire coil-to-globule transition based on the hydrodynamic size.

In plots of $\alpha_s^3|\tau|M_w^{1/2}$, each polymer/solvent system showed an asymptotic height in the collapsed regime based on $R_g$. The prefactor $(A^*N_1)$, determined according to eq 8, depends strongly upon the chemical nature of the solvent and the solvent quality (i.e., good or poor). The theoretical insight on the detailed mechanism of the coil collapse and a reinterpretation on the $A^*$ parameter are suggested.

It is interesting to calculate the value of the expansion factor, $\alpha_s$, at the temprature where the collapsed regime based on $R_g$ first takes place. Surprisingly, almost the same $\alpha_s$ value of $\sim 0.86 \pm 0.02$ was obtained for all PS/solvent systems. If we assume that the collapsed state is achieved when the leading term, $w/\alpha^3 a^6$ in eq 1 is larger than the other term, $|\alpha^5 - \alpha^3|$, by a factor of 20 (corresponding to a $\sim 5\%$ error in our measurements of $|\tau|M_w^{1/2}$), the $y$ value, as the ratio of third virial coefficient ($w$) to the square of one segmental volume ($a^6$) becomes $\sim 2.0$ from the equation $y = 20|\alpha^5 - \alpha^3|\alpha^3$. This implies that the third virial coefficient, $w$, is independent of the chemical nature of the solvent for a given polymer in agreement with an earlier assumption in deriving $\alpha \sim (|\tau|N^{1/2})^{1/3}$. It still remains an interesting topic to observe experimentally how the parameter $y$ varies with the structure of the side group in the polymer and the flexibility of the polymer chain.

**Acknowledgment.** We gratefully acknowledge support of this research by the National Science Foundation, Polymers Program (DMR 8617820).

**Registry No.** PS, 9003-53-6; MA, 79-20-9; 2,6-di-*tert*-butyl-4-methylphenol, 128-37-0.

## References and Notes

(1) Prigogine, I. *The Molecular Theory of Solutions*; North Holland: Amsterdam, 1957.
(2) Delmas, G.; Patterson, D.; Somcynsky, T. *J. Polym. Sci.* **1962**, *57*, 79.
(3) Patterson, D. *J. Polym. Sci., Part C* **1968**, *16*, 3379.
(4) Patterson, D.; Delams, G. *Discuss. Faraday Soc.* **1970**, *49*, 98.
(5) Patterson, D. *Macromolecules* **1969**, *2*, 672.
(6) Slagowski, E.; Tsai, G.; McIntyre, D. *Macromolecules* **1976**, *9*, 687.
(7) Nierlich, M.; Cotton, J. P.; Farnoux, B. *J. Chem. Phys.* **1978**, *69*, 1379.
(8) Bauer, D. R.; Ullman, R. *Macromolecules* **1980**, *13*, 392.
(9) Pritchard, M. J.; Caroline, D. *Macromolecules* **1980**, *13*, 957.

(10) Swislow, G.; Sun, S. T.; Nishio, I.; Tanaka, T. *Phys. Rev. Lett.* **1980**, *44*, 796.
(11) Sun, S. T.; Nishio, I.; Swislow, G.; Tanaka, T. *J. Chem. Phys.* **1980**, *73*, 5971.
(12) Miyaki, Y.; Fujita, H. *Polym. J.* **1981**, *13*, 749.
(13) Oyama, T.; Shiokawa, K.; Baba, K. *Polym. J.* **1981**, *13*, 167.
(14) Stapanek, P.; Konak, C.; Sedlacek, B. *Macromolecules* **1982**, *15*, 2141.
(15) Perzynski, R.; Adam, M.; Delsanti, M. *J. Phys. (Les Ulis, Fr.)* **1982**, *43*, 129.
(16) Perzynski, R.; Delsanti, M.; Adam, M. *J. Phys. (Les Ulis, Fr.)* **1984**, *45*, 1765.
(17) Vidakovic, P.; Rondelez, F. *Macromolecules* **1984**, *17*, 418.
(18) Selser, J. C. *Macromolecules* **1985**, *18*, 585.
(19) Park, I. H.; Wang, Q.-W.; Chu, B. *Macromolecules* **1987**, *20*, 1965.
(20) Saeki, S.; Konno, S.; Kuwahara, N.; Nakata, M.; Kaneko, M. *Macromolecules* **1974**, *7*, 521.
(21) Kubota, K.; Abbey, K. M.; Chu, B. *Macromolecules* **1983**, *16*, 137.
(22) De Gennes, P.-G. *J. Phys. Lett.* **1975**, *36*, L55.
(23) Sanchez, I. C. *Macromolecules* **1979**, *12*, 980.
(24) Akcasu, A. Z.; Han, C. C. *Macromolecules* **1979**, *12*, 276.
(25) Farnoux, B.; et al. *J. Phys. (Les Ulis, Fr.)* **1978**, *39*, 77.
(26) Huglin, M. B., Ed. *Light Scattering from Polymer Solutions*; Academic: New York, 1972.
(27) Chu, B. *Laser Light Scattering*; Academic: New York, 1974.
(28) Berne, B. J., Pecora, P., Eds. *Dynamic Light Scattering*; Wiley: New York, 1976.
(29) Stockmayer, W. H.; Schmidt, M. *Pure Appl. Chem.* **1982**, *54*, 407.
(30) Schmidt, M.; Burchard, W. *Macromolecules* **1981**, *14*, 210.
(31) Washburn, E. W., Ed. *International Critical Tables of Numerical Data, Physics, Chemistry and Technology*; McGraw-Hill: New York, 1926.

# Influence of Solvent Casting on the Evolution of Phase Morphology of PC/PMMA Blends

**Jeanne M. Saldanha and Thein Kyu***

*Center for Polymer Engineering, The University of Akron, Akron, Ohio 44325.*
*Received February 20, 1987*

ABSTRACT: The effect of solvent casting on the structure evolution of bisphenol A polycarbonate (PC) and polymethyl methacrylate (PMMA) mixtures has been investigated as a function of solvent evaporation rate, casting temperatures, and the kind of solvent used. The casting conditions exert profound effects on the final blend morphology. PC/PMMA blends cast from tetrahydrofuran (THF) at low temperatures (20 °C or below) exhibit phase separation behavior as well as solvent-induced crystallization in the PC phase. The solvent casting at ambient (23 °C) shows the development of a modulated biphase structure with high level of interconnectivity characteristic of spinodal decomposition. However, the casting at an elevated temperature (47 °C) yields transparent amorphous films with a single glass transition ($T_g$) located at intermediate temperatures between those of pure polymers and varies systematically with composition. Cloud-point measurements on the PC/PMMA system reveal a miscibility window reminiscent of an LCST (lower critical solution temperature). Solvent casting of PC/PMMA blends from cyclohexanone (CHN) generally results in phase separation accompanied by crystallization of the PC phase. The casting from methylene chloride (MC) shows no indication of solvent-induced crystallization, but the system phase separates during solvent evaporation. The mechanisms of phase separation and crystallization during solvent evaporation have been investigated by means of time-resolved light scattering, and the results are analyzed in the context of a pseudobinary approximation.

## I. Introduction

Thermodynamic and kinetic studies of polymer phase separation[1-9] have made considerable progress. However, the general perception is that most polymer pairs are immiscible as a result of low entropy of mixing associated with long molecular structures of polymers. This notion has changed gradually since polymer miscibility can be enhanced through some specific interactions between dissimilar molecules. Additional factors such as blending conditions were found to play an important role in miscibility studies.[10] A number of mixing techniques have been employed in the preparation of polymer blends, among which mechanical mixing and solvent blending are common methods widely practiced in industries and many laboratories. It is, however, difficult to obtain homogeneous polymer mixtures with the former method. The latter method generally gives a better mix. Even in solvent blending, several techniques, namely, solution casting, freeze drying, or coprecipitation have been adopted as can be witnessed in the literature.[1-12] Little attention has been paid to the detailed procedure; however, this turns out to be very important according to the recent studies.[10,11,13]

Varnell and co-workers[10] demonstrated the effect of solvent casting on crystallization and miscibility of polycarbonate (PC)/polycaprolactone (PCL) blends. They found that when PC/PCL were cast from tetrahydrofuran (THF), PC phase resulted in crystallization, whereas the casting from methylene chloride (MC) showed no sign of crystallization in PC phase. This behavior has been attributed to differences in the rate of solvent evaporation and the interaction between solvents and polymers. The authors concluded that the strong interaction (the hydrogen bonding) was responsible for miscibility enhancement in PC/PCL blends.

The development of modulated structure during solvent casting of polymer blends was reported recently by Inoue et al.[11] on many polymer blend systems, typically poly(methyl methacrylate)/poly(acrylonitrile-*co*-styrene) and poly(vinyl methyl ether)/polystyrene having a lower critical solution temperature (LCST) and poly(methylphenylsiloxane)/polystyrene having an upper critical solution temperature (UCST). They reached a conclusion that the modulated structure resulted from the spinodal decomposition during solvent casting of the ternary blend solution. The thermodynamic aspects of spinodal decomposition have been interpreted in accordance with the procedure of Zeeman and Patterson.[12]

The kinetics of phase separation and phase dissolution of ternary blend solutions were also reported by Hashimoto et al.[13] on polystyrene/styrene–butadiene diblock poly-

0024-9297/87/2220-2840$01.50/0 